Proceedings of the
47th IEEE Conference on Decision and Control
Cancun, Mexico, Dec. 9-11, 2008

Six Degree of Freedom Variable Hierarchy Sliding Mode Control in Halo Orbits With Potential Function Guidance

N K Lincoln and S M Veres

Abstract— **This paper presents a variable hierarchy six degree of freedom non-linear sliding mode controller for a satellite using potential function guidance for both position and attitude. The novelty is the formulation of the joint attitude/position sliding mode controller in combination with potential function guidance and proof of its asymptotic stability. The control method scales well to multiple satellites flying in formation with dynamic position and attitude requirements and as such is highly relevant to application in space systems such as interferometry. A target application of the acquisition and maintenance of a Halo type orbit about an unstable collinear Lagrange point, to a specified attitude, is obtained under the influence of the restricted three body dynamics.**

I. INTRODUCTION

A Lagrange point (referred to herein as a Liberation point) is an equilibrium solution to Euler's classic restricted three body problem (RTBP). It is a location where the gravitational and centrifugal forces acting on a third body are balanced. Fig. 1 depicts the Liberation Points of the RTBP, where the points L_1, L_2 and L_3 are collinear with the primary system bodies; points L_4 and L_5 form the so-called 'equilateral' points with the system primaries. The existence and the complex dynamics in the vicinity of these points has been of great mathematical interest since Poincaré's early work in 1899, the three volumes of *Méthodes Nouvelles*. Szebelehely's treatise [1] was the first publication to amalgamate the work completed by numerous mathematicians into a comprehensive document covering the theoretical aspects of Liberation point locations and the existence of achievable orbits about these points.

The use of satellites in Liberation Point orbits have been investigated since the pioneering text by Farquhar [2] in which the use of a satellite positioned in an orbit about the L_2 point of the Earth-Moon system was suggested to permit radio communications on the dark side of the moon. Liberation point satellites have been flown, the International Solar Earth Explorer-3 ($ISEE-3$) and the Solar and Heliospheric Observatory (SOHO) missions being the most famous of these [30][31]. More recently, the use of liberation point orbits has been highlighted as an ideal location for satellite imaging formations such as Herschel[27], the Terrestrial Planet Finder (TPF)[28] and the Micro Arc-Second X-ray Imaging Mission (MAXIM)[29]. Individual platforms, such as Herschel and SOHO, require accurate control of both position and attitude throughout the entirety of the intended orbit; interferometric platforms such as the TPF have the added complexity of formation flight requirements.

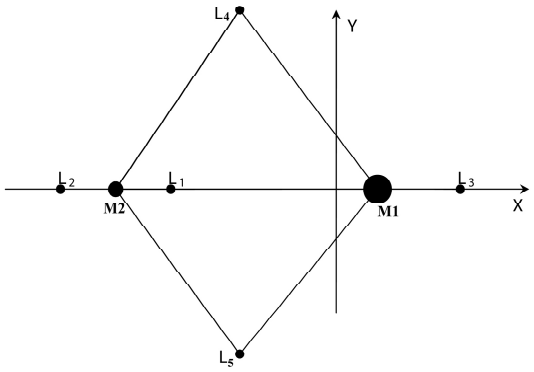

Fig. 1. Liberation Points of the RTBP

For such space systems where there is a significant time delay in Earth based communications, autonomy becomes important; where autonomy here relates to autonomous movement in space/time. For formation flying systems this autonomy is essential for operation. In addition to autonomy requirements, the need for a six degree of freedom control system is inherent due to the need for acquisition of time varying positions and attitudes. The combined six degree of freedom dynamics of rigid body, where both attitude and position translation are considered, is non-linear in nature and as such traditional linear control theory is difficult to apply.

Control solutions for satellite motion within the three-body environment have been presented by numerous authors. Howell, who's early work included numerical determination of periodic Halo orbits[3], presents a control methodology based on a Floquet control law within [5], an extension of the work presented by Gómez et al [6]. The Floquet approach is a method for countering disturbances to enable positional maintenance in the vicinity of a prescribed Halo orbit and does not consider attitude control or manoeuvres to achieve a specified configuration. More complete solutions are presented by [7] and [8]. [8] presents a hierarchical optimal control solution to provide attitude and position control through reducing a set of requirements to a minimisation problem. Although permitting both attitude and position

This work was supported in part by the EPSRC

N K Lincoln is with School of Engineering Sciences, University of Southampton, United Kingdom. nkl@soton.ac.uk

S M Veres is with School of Engineering Sciences, University of Southampton, United Kingdom. smv@soton.ac.uk

control, the method does not allow for collision avoidance considerations; a factor acknowledged by the author. An important result from [8], is that the decentralised scheme is able to cope with a complex set of requirements, where a monolithic scheme would fail. [7] presents an adaptive output feedback control scheme for a leader-follower configuration in which a follower satellite is tasked with following a halo reference trajectory. [7] uses a velocity filter to provide estimates of relative velocities and as such allows for control using only relative positional measurements. The control regime is however, only prescribed for a leader-follower configuration to the n^{th} order and attitude manoeuvres are not considered. General control schemes, not applied within the RTBP regime, exist in the form of [9],[10] both of which use a potential function guidance method combined with sliding mode control for position control, but neither consider attitude manoeuvres in conjunction with positional movement. Numerous papers exist for formation flight in the Low Earth Orbit, though very few consider the combined nonlinear position and attitude control. Indeed, the main author in this area [12],[13] is the same for [7], in which the same leader-follower controller is implemented within a new dynamical regime. [14] presents a combined sliding mode controller for both attitude and position in the presence of zero disturbance and without guidance. Perhaps the richest resource for combined position and attitude control schemes lay in the field of Autonomous Underwater Vehicles, such as [15], which develops a class of non-linear PD control laws using a Lyapunov approach and tested by step response commands.

Autonomous guidance, or path planning, is a complex issue which is exacerbated with increasing formation elements. For true autonomous operation, each formation element, herein referred to as *'agent'*, is required to regulate both its position and attitude within the group of agents based on its own percepts. [25] presents a broad introduction to the field of multi-agent systems and highlights the complexity of agent action selection. Several solutions to the agent action selection problem for robotic navigation, spacecraft proximity with rendezvous and self assembly of space based structures exist in the form of potential functions, dynamic systems theory and optimal control theory [16],[17],[9]. The most developed of these is the method of potential functions in which an artificial potential field is created from agent percepts and subsequently used to model an agents' time-varying environment. Within this model the action selection is prescribed by following the local gradient of the potential field. Conceptually this is a very simple approach but can lead to the acquisition of an undesirable local minimum equilibrium position by an agent. Solutions to this problem have been suggested by numerous sources, including the implementation of random walks[18] and forming the potential field using Laplacian or harmonic functions[19][20]. An elegant solution to the satellite agent collaboration problem using potential functions is presented by [9] and [10]. In the latter, the method is referred to as equilibrium shaping. This technique is an amalgamation of various methods used within robot path planning and AI in which a kinematic field is constructed as the sum of different weighted potential field contributions. These contributions, or behaviors, result in a global swarm behavior which solve a target assignment problem autonomously.

In this paper, a potential field method is combined with a novel variable hierarchy six degree of freedom sliding mode controller for autonomous satellite operation in an unstable halo orbit. A single agent is deployed into a leader-follower configuration to track a desired orbital trajectory whilst obtaining and maintaining a desired attitude. Although only a single agent is deployed in this scenario, the method is scalable to n agents deployed into a time varying large scale formation. The main contribution of this paper is a novel methodology for solving the joint spacecraft guidance, attitude and position control problem.

Section II develops the equations of motion for the RTBP environment and a rigid body with six degrees of freedom. Section III develops the guidance and control laws which are simulated in Section IV. The paper is concluded with an outline of future work and a summary of the simulation results obtained.

II. Dynamics

The development of the dynamics and kinematics will be based upon a single agent, considered to be holonomic with respect to control. In addition, the notation will be as follows:

- Capital Letter, Bold Face = Matrix, $\mathbf{A}$
- Lower case letter, Bold Face = Vector, $\mathbf{a}$
- Lower case letter, italic = Scalar, a
- m=mass,
- $\mathbf{v}$=velocity, $[v_x, v_y, v_z]^T$
- ω=angular velocity, $[\omega_x, \omega_y, \omega_z]^T$
- $\mathbf{f}$=force, $[f_x, f_y, f_z]^T$
- τ=torque, $[\tau_x, \tau_y, \tau_z]^T$
- $\mathbf{J}$= inertial matrix

A. Lagrange Point Dynamics

[1],[23] give a detailed development of both the circular restricted three-body problem and the elliptic restricted three-body problem, which includes periodic distance variation between the two primary bodies.

Referring to Fig. 2 where m_1 and m_2 represent the bodies of significant mass and m represents the third (insignificant) body. Vector R is the distance from the system barycenter to the third body and vectors r_1 and r_2 are the distances from the significant masses to the third body. For the circular restricted problem, where the orbital motion of the two primary bodies about their barycenter is assumed circular and resulting in a system with a constant orbital velocity, it is shown in [23] that the non-dimensional equations of motion, where distances are in units of D and time in units of $1/n$, resultant from inertial and gravitational acceleration are given by (1).

$$\begin{aligned} \ddot{x}-2\dot{y}-x &= -\frac{(1-\rho)(x-\rho)}{r_1^3}-\frac{\rho(x+1-\rho)}{r_2^3} \\ \ddot{y}+2\dot{x}-y &= -\frac{(1-\rho)y}{r_1^3}-\frac{y\rho}{r_2^3} \\ \ddot{z} &= -\frac{(1-\rho)z}{r_1^3}-\frac{z\rho}{r_2^3} \end{aligned} \quad (1)$$

where

$$\begin{aligned} r_1 &= \sqrt{(x-\rho)^2+y^2+z^2} \\ r_2 &= \sqrt{(x+1-\rho)^2+y^2+z^2} \\ n &= \sqrt{\frac{G(m_1+m_2)}{D^3}} \end{aligned}$$

with ρ representing the mass ratio of a two body system as

$$\rho = \frac{m_2}{m_1+m_2}$$

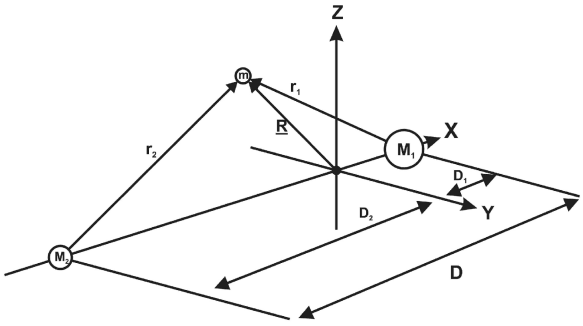

Fig. 2. Schematic Overview of the RTBP

B. Six Degree of Freedom Dynamics

The non-linear rigid body six degree of freedom dynamics are well documented. Using Newton/Euler equations to resolve for forces and moments respectively, we generate the translational and rotational motion equations for a rigid spacecraft:

$$m\dot{\mathbf{v}}+m\mathbf{\Omega}\mathbf{v}=\mathbf{f} \quad (2)$$

$$\mathbf{J}\dot{\omega}+\mathbf{\Omega}\mathbf{J}\omega=\boldsymbol{\tau} \quad (3)$$

where the skew symmetric matrix $\mathbf{\Omega}$ represents the angular velocity cross product matrix as is given by (4).

$$\mathbf{\Omega}=\begin{bmatrix} 0 & -\omega_3 & \omega_2 \\ \omega_3 & 0 & -\omega_1 \\ -\omega_2 & \omega_1 & 0 \end{bmatrix} \quad (4)$$

The kinematic equation describing the evolution of the spacecraft position and orientation are given by (5).

$$\dot{\mathbf{d}} = -\mathbf{\Omega}\mathbf{d}+\mathbf{v} \quad (5)$$

$$\dot{\mathbf{q}} = \tfrac{1}{2}\widetilde{\mathbf{\Omega}}\mathbf{q} \quad (6)$$

where

$$\widetilde{\mathbf{\Omega}}=\begin{bmatrix} 0 & \omega_3 & -\omega_2 & \omega_1 \\ -\omega_3 & 0 & \omega_1 & \omega_2 \\ \omega_2 & -\omega_1 & 0 & \omega_3 \\ -\omega_1 & -\omega_2 & -\omega_3 & 0 \end{bmatrix} \quad (7)$$

$\mathbf{d}$ represents the satellite position in the body frame and $\mathbf{q}$ is the quaternion vector.

A complete representation of the dynamics and kinematics for a single rigid body is given by (8).

$$\begin{aligned} \tfrac{d}{dt}\begin{bmatrix} \mathbf{d} \\ \mathbf{v} \\ \mathbf{q} \\ \omega \end{bmatrix} &= \begin{bmatrix} -\mathbf{\Omega}\mathbf{d}+\mathbf{v} \\ -\mathbf{\Omega}\mathbf{v} \\ \tfrac{1}{2}\widetilde{\mathbf{\Omega}}\mathbf{q} \\ -\mathbf{J}^{-1}\widetilde{\mathbf{\Omega}}\mathbf{J}\omega \end{bmatrix} + \\ &\quad \begin{bmatrix} \mathbf{0}_{(3,3)} & \mathbf{0}_{(3,3)} \\ m^{-1}\mathbf{I}_{(3,3)} & \mathbf{0}_{(3,3)} \\ \mathbf{0}_{(4,3)} & \mathbf{0}_{(4,3)} \\ \mathbf{J}^{-1}\mathbf{\Phi}_{(3,3)} & \mathbf{J}^{-1} \end{bmatrix}\begin{bmatrix} \mathbf{f} \\ \tau \end{bmatrix} + \\ &\quad \begin{bmatrix} \mathbf{0}_{(3,3)} & \mathbf{0}_{(3,3)} \\ m^{-1}\mathbf{I}_{(3,3)} & \mathbf{0}_{(3,3)} \\ \mathbf{0}_{(4,3)} & \mathbf{0}_{(4,3)} \\ \mathbf{0}_{(3,3)} & \mathbf{J}^{-1} \end{bmatrix}\begin{bmatrix} \mathbf{f}_d \\ \tau_d \end{bmatrix} \\ \dot{\mathbf{x}} &= f(\mathbf{x})+\mathbf{B}\mathbf{u}+\mathbf{C}\mathbf{u}_d \end{aligned} \quad (8)$$

where $\mathbf{\Phi}$ is the cross product of control torques, a consequence of actuator misalignment resulting in parasitic torques generated from translational impulses. For subsequent analysis $\mathbf{\Phi}$ will be taken as $\mathbf{0}_{(3,3)}$. $\mathbf{u}$ is the vector of applied control $[force, torque]^T$ and $\mathbf{u}_d$ is a vector representing external force and torque disturbances. Rows 3-6 and 11-13 of matrix $\mathbf{B}$ will be joined together to form a squared non-singular sub-matrix $\mathbf{B}^*$ that will be used later in Section 3.2 in the formulation of the sliding mode equivalent control term $\mathbf{u}_{eq}$.

III. Guidance and Control

Guidance for the desired agent state will be provided through the use of potential functions in a similar manner to the method within [10] but with the added novelty of providing potential functions for attitude guidance. Separate potential functions will be used to prescribe desired velocity vectors for both position and attitude in the form of $\mathbf{\Psi}\mathbf{v}_d$ and $\mathbf{\Psi}\omega_d$, where $\mathbf{\Psi}$ is the inertial to body conversion matrix. Using the actual velocity vectors, $\mathbf{v}$ and ω, in combination with the desired velocity vectors, a feedback regime will be based upon the velocity vector errors:

$$\begin{aligned} \mathbf{v}_e &= \mathbf{v}-\mathbf{\Psi}\mathbf{v}_d \\ \omega_e &= \omega-\mathbf{\Psi}\omega_d \end{aligned}$$

which will be used within the sliding mode control regime presented within Section III-B. Prior to this, within Section III-A, the potential functions used to achieve the desired guidance for position and attitude will be developed. Within Section III-C, the developed controller is generalised for a group of n agents.

A. Guidance Law- Potential Functions

The potential function used as guidance for position will be constructed as a function of the agent distance from a desired point in space, referred to as a sink location. Such a gathering behavior results in a predominantly global influence over the agent. A compound potential, formed by introducing n attractors towards the n sinks, ε_j can be used. A general expression for the negative gradient of a potential function which is prescribing a gathering behavior of agent i to sink ε_j is

$$\Upsilon_i^{gather} = \sum a_j \cdot \|(\varepsilon_j - \mathbf{x}_i)\| \cdot (\varepsilon_j - \mathbf{x}_i)$$

where a_j is an integer coefficient dependant on the sink priority. For the instance of leader-follower position tracking control, only a single sink location is required for each follower agent.

In considering more than one agent, collision avoidance becomes an integral part of the control requirements. A collision avoidance constraint can be imposed upon an agent by the introduction of an inter-agent avoidance potential between agent i and agent j given in [9] as

$$\Upsilon_i^{avoid} = -b_i \sum_j (\mathbf{x}_j - \mathbf{x}_i)\, exp\left(-\frac{\|\mathbf{x}_j - \mathbf{x}_i\|}{k_i}\right),$$

b_i is a suitable weighting parameter and k_i represents an additional weighting parameter dictating the sphere of influence for the given avoid behaviour.

The potential function used as guidance for rotational position will be constructed as a function of the agent orientation error from a desired orientation in space, using the quaternion notation. The error quaternion, $\mathbf{q}_e$, is given within [26] as:

$$\mathbf{q}_e = \mathbf{Q}_d \mathbf{q}$$

where $\mathbf{Q}_d$ is the matrix multiplication of the desired quaternion vector, $\mathbf{q}_d$, obtained by using the components of $\mathbf{q}_d$:

$$\mathbf{Q}_d = \begin{bmatrix} q_{d4} & q_{d3} & -q_{d2} & q_{d1} \\ -q_{d3} & q_{d4} & -q_{d1} & q_{d2} \\ q_{d2} & -q_{d1} & q_{d4} & q_{d3} \\ -q_{d1} & -q_{d2} & -q_{d3} & q_{d4} \end{bmatrix}$$

There exists a one-to-one equivalence between the direction cosine matrix elements and the elements of the quaternion vector and so a suitable output potential function can be based on a desired orientation can be represented in the following form.

Definition Using the attitude reference $\mathbf{q}_d$ as a sink an attitude reference guidance vector for ω is defined as

$$\Upsilon_i^{orient} = c_i \cdot q_{e_4} \cdot \begin{bmatrix} q_{e_1} \\ q_{e_2} \\ q_{e_3} \end{bmatrix},$$

where c_i represents a weighting factor.

Alike the positional potential function development, the potential function for required attitude could consist of multiple weighted parameters to result in a more complex behavior dependant on the environmental percepts. In the presented scenario, only the acquisition of a specified attitude is considered.

The overall position and angular velocity reference for agent i can then be defined as the sum of all partial contributions as:

$$\mathbf{\Gamma}_i = \begin{bmatrix} \mathbf{v}_d \\ \omega_d \end{bmatrix} = \begin{bmatrix} \Upsilon_i^{gather} + \Upsilon_i^{avoid} \\ \Upsilon_i^{orient} \end{bmatrix} \tag{9}$$

B. Sliding Mode Control Development

The starting point for developing sliding mode control is the selection of a suitable sliding surface, σ, such that when $\sigma = 0$ is reached, the system exhibits the desired motion. For the purposes of a combined position and attitude controller, two separate sliding surfaces are required relating to the separate translational and rotational movements.

$$\begin{aligned} \sigma_1 &= k_v \cdot \mathbf{v}_e \\ \sigma_2 &= k_a \cdot \omega_e \end{aligned}$$

With k_v and k_a representing fixed scalar gains for velocity and attitude respectively. These gain values are used to scale the magnitude of force and torque control signals by scaling of the sliding mode inputs generated by the potential functions. The above sliding surfaces can be placed into matrix form:

$$\begin{aligned} \mathbf{\Sigma} &= [\sigma_1, \sigma_2]^T \\ &= \begin{bmatrix} k_v \cdot \mathbf{I}_{(3,3)} & \mathbf{0}_{(3,3)} \\ \mathbf{0}_{(3,3)} & k_a \cdot \mathbf{I}_{(3,3)} \end{bmatrix} \begin{bmatrix} \mathbf{v}_e \\ \omega_e \end{bmatrix} \\ &= \mathbf{K}\mathbf{x}_e \\ &= \mathbf{K} \cdot [\mathbf{x} - \mathbf{\Psi} \cdot \mathbf{x}_d] \end{aligned} \tag{10}$$

Traditionally, hierarchical sliding mode control is employed by driving a single sliding surface to zero within finite time and then progressing sequentially through the set of sliding modes whilst maintaining preceding modes until $\sum \sigma_i \equiv 0$, $i = 1, 2, ..., n$. Due to the nature of this approach, hierarchical sliding mode control is also referred to as a fixed order switching scheme [21][22]. Such a method is limited in that the prescribed order of reaching sliding modes may not be ideal and can result in a large magnitude in control effort. In contrast, a 'free-order' sliding mode process operates on a first-reach-first-switch scheme in which the order of sliding modes is not specified. Although possessing more desirable dynamical characteristics, by definition no direct control is available over sliding modes; this can be disadvantageous

in cases when a precedence is required due to actuation limitations.

A modified hierarchical scheme is presented in (11), where $\alpha_1 + \alpha_2 \equiv 1$. By modifying the positive definite α_i variables, the sliding mode scheme can progress in various ways. When $\alpha_1 = \alpha_2$ the scheme will progress as a 'free-order' method. When $\alpha_1 \neq \alpha_2$ a hierarchical scheme can be imposed. The magnitudes of the α_i variables are evaluated within the guidance functions as a function of error velocities and mode priorities. If control saturation is approaching, a precedence operation over position and attitude can impose appropriate α_i values; at other times a 'free-order' scheme is followed.

$$\begin{aligned} \varsigma &= \begin{bmatrix} \alpha_1 \cdot \mathbf{I}_{3,3} & 0_{3,3} \\ 0_{3,3} & \alpha_2 \cdot \mathbf{I}_{3,3} \end{bmatrix} \begin{bmatrix} \sigma_1 \\ \sigma_2 \end{bmatrix} \\ &= \mathbf{\Lambda} \cdot \mathbf{\Sigma} \end{aligned} \tag{11}$$

Using the theory of variable structure systems [21],[22], an equivalent control term is determined such that when on the sliding surface, motion is constrained to the surface $\sigma_i = 0$ for all time having intercepted the manifold. Applied to the sliding modes outlined in (10), we require that $\mathbf{\Sigma} = 0$ and $\dot{\mathbf{\Sigma}} = 0, \forall t \geq t_0$ where t_0 is the time of manifold intersection. For the multi-input/multi-output case, this is satisfied by

$$\mathbf{u}_{eq} = \mathbf{B}^{*-1} \left(\mathbf{\Psi} \dot{\mathbf{x}}_d - \mathbf{f}(x) \right) \tag{12}$$

The equivalent control term, $\mathbf{u}_{eq}$, given in (12) must be augmented with a switching term, $\mathbf{u}_{sw}$, to guarantee convergence to the sliding surface. Defining a positive definite Lyapunov function candidate as

$$V(\varsigma) = \frac{\varsigma^T \cdot \varsigma}{2}, \tag{13}$$

for asymptotic stability we require that $\dot{V}(\varsigma) \leq 0 \ \forall \ t$. Using (8), (11) and (13) we can show that

$$\begin{aligned} \dot{V}(\varsigma) &= \varsigma \cdot^T \dot{\varsigma} \\ &= \varsigma \left(\mathbf{\Lambda} \cdot \mathbf{K} \left(\mathbf{f}(x) + \mathbf{B}\mathbf{u} \right) - \mathbf{\Lambda} \cdot \mathbf{K} \cdot \mathbf{\Psi} \dot{\mathbf{x}}_d \right) \end{aligned}$$

By substitution of $\mathbf{u} = u_{eq} + u_{sw}$ it follows that the switching term

$$\mathbf{u}_{sw} = -\mathbf{B}^{*-1} \cdot \mathbf{K}^{-1} \cdot \mathbf{\Lambda}^{-1} \cdot sgn(\varsigma),$$

satisfies

$$\begin{aligned} \dot{V}(\varsigma) &= -\varsigma^T sgn(\varsigma) \\ &= -\|\varsigma\|_1 \\ &\leq 0 \ \forall t \end{aligned}$$

and hence the high level sliding mode, ς, is asymptotically stable. The following result has been obtained.

Theorem 3.1: For constant velocity references $\mathbf{v}_d$, ω_d the sliding mode controller

$$\begin{aligned} \mathbf{u}_i &= \mathbf{u}_{i_{eq}} + \mathbf{u}_{sw} \\ &= \mathbf{B}^{*-1} \left(\mathbf{\Psi} \cdot \dot{\mathbf{x}}_d - \mathbf{f}(x) \right) - \mathbf{B}^{*-1} \cdot \mathbf{K}^{-1} \mathbf{\Lambda}^{-1} \cdot sgn(\varsigma) \end{aligned}$$

is asymptotically stable.

To prevent excessive chattering due to the theoretical infinite switching frequency associated with the sign function, it is conventional to use a boundary layer solution in close proximity to the switching surface. This is achieved by replacing the sign function with a saturation function in which

$$\text{sat}(y) = \begin{cases} y & \text{if} |y| \leqslant 1 \\ sgn(y) & \text{otherwise} \end{cases}$$

C. Sliding Mode Control For n Agents

In considering the complete potential function guidance law for agent i given by (9), the control response for each agent will be

$$\begin{aligned} \mathbf{u}_i &= \mathbf{u}_{i_{eq}} + \mathbf{u}_{i_{sw}} \\ &= \mathbf{B}^{*-1}_i \left(\mathbf{\Psi}_i \cdot \dot{\mathbf{x}}_{i_d} - \mathbf{f}_i(x) \right) - \mathbf{B}^{*-1}_i \cdot \mathbf{K}_i^{-1} \mathbf{\Lambda}_i^{-1} \cdot sat(\varsigma_i) \end{aligned}$$

with

$$\varsigma_i = \mathbf{\Lambda}_i \cdot \mathbf{\Sigma}_i$$

to regulate the agent to a desired position and attitude using coordinated potential function gradients suitable for the intended mission application. Each agent defines its own potential gradient for translational and attitude velocities and the sliding mode control solution developed in this paper can be applied.

IV. Simulation Results

The controller in combination with the potential function guidance given in Section III was coded using *MATLAB*®. The required halo orbit to be followed, equivalent to following a leader satellite, was that of the ISEE-3 mission about the L_1 liberation point using orbital data generated by an analytical third order Richardson approximation [4]. Insertion into the orbit was assumed to occur with random but bounded velocity, position and attitude errors. The controller objective was to regulate both orbital location and attitude with respect to the reference trajectory. Orbital dynamics were simulated using the three body dynamics presented in Eqn. 1. Within the simulations realistic external disturbance were introduced using random, uniformly distributed zero mean variables bounded between $\pm 5\mu N$ and $\pm 0.5\mu Nm$ for both force and torque respectively. Control actuation is assumed holonomic and bounded to realistic thrust and torque levels, with a maximum levels of $1mN$ and $1mNm$ respectively for a spacecraft mass of 10kg.

Fig. 3 shows the time evolution of the position error when the satellite trajectory is regulated to the desired orbit. Fig. 4 shows the associated quaternion component output over the same time period; the bottom plot is a verification plot to visualise the $\sum q_i^2$ output, which mathematically should be unity. The modified hierarchical sliding surface components for position and orientation are shown in Figs. 5 and 6.

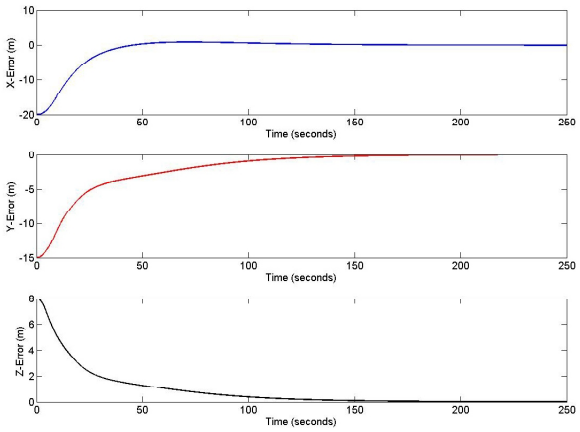

Fig. 3. Time Variation of Position Errors in [x,y,z]

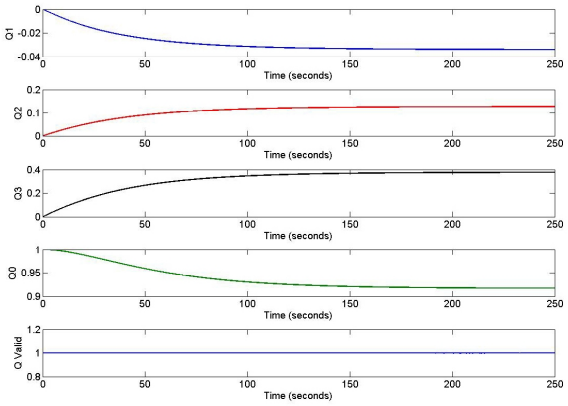

Fig. 4. Time Variation of Quaternion vector $[q_{(1-3)}, q_0]$

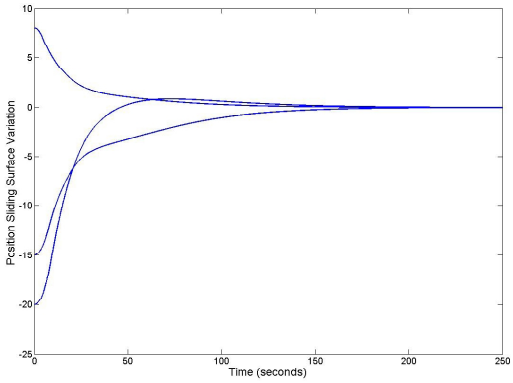

Fig. 5. Positional Sliding Surface Time Response

Fig. 7 shows both the controlled and uncontrolled orbital positions, subject to the random orbital insertion conditions. It is clear that the uncontrolled orbit degrades significantly within a single orbit, corresponding to a time period of 177.73 days, whereas the controlled orbit maintains the desired orbit at the desired attitude.

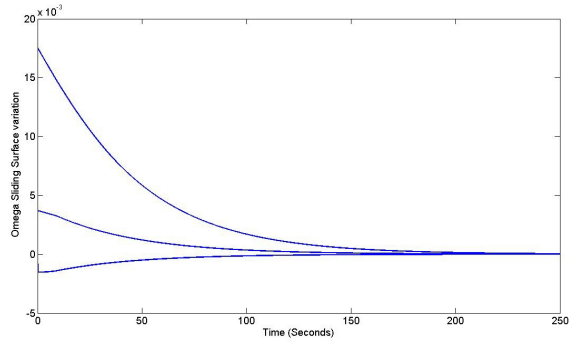

Fig. 6. Angular Velocity Sliding Surface Time Response

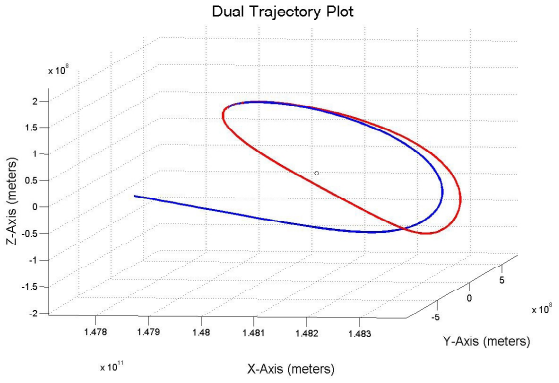

Fig. 7. Regulated and Unregulated Satellite Orbits

V. Conclusions

A variable hierarchy sliding mode controller has been presented in conjunction with a guidance method which is scalable to n agents. Control of a single agent has been demonstrated, with the agent regulated to a halo type orbit generated using a Richardson approximation. Future work is to include a discrete time implementation of the controller expanded to a group of agents tasked with achieving a predefined configuration, whilst following a differentially corrected orbit. In addition to the discretisation of the control system, disturbance torques and forces will also be considered.

VI. Acknowledgments

The author would like to thank Dr C. Bramanti and Dr D. Izzo for their assistance and guidance whilst at the European Space Technology Research Centre, from which the presented work originated.

REFERENCES

[1] V. Szebelehely, Theory of Orbits: the Restricted Three Body Problem, *Academic Press- 1967*, ASIN: B0000CNN4X

[2] R.W. Farquhar, The Control And Use of Liberation Point Satellites, *NASA Technical Report R* – 346, 1970.

[3] K.C. Howell, Three Dimensional Periodic 'Halo' Orbits, *Celestial Mechanics* 32,1984, pp 53-71.

[4] D.L. Richardson, Analytic Construction Of Periodic Orbits About The Collinear Points, *Celestial Mechanics* 22, 1982, pp 241-253.

[5] K.C. Howell and L.D. Millard, Control of Satellite Imaging Formations in Multi-Body Regiems, 57^{th} *International Astronautical Congress*, Valencia Spain, 2006.

[6] G. Gómez, K.C. Howell, J. Masdermount, and C. Simó, Station Keeping Strategies for Translunar Liberation Point Orbits, *Advances in Astronautical Sciences*, Vol. 99, Pt.2, 1998, pp. 949-967.

[7] H. Wong and V. Kapila, Spacecraft Formation Flying Near Sun-Earth L_2 Lagrange Point: Trajectory generation and Adaptive Output Feedback Control, *2005 American Control Conference*, Portland, USA.

[8] O. Junge, J.E. Marsden and S. Ober-Blöbaum, *Optimal Reconfiguration of Formation Flying Spacecraft- a Decentralised Approach*, Proceedings of the 45^{th} IEEE Conference on Descision and Control, 2006, San Diego, USA.

[9] V. Gazi, Swarm Aggregations Using Artificial Potentials and Sliding Mode Control, *Proceedings of the IEEE Confereence on Descision and Control*, IEEE Publications, Dec. 2003, pp 2848-2853.

[10] D. Izzo and L. Pettazzi, Autonomous and Distributed Motion Planning for Satellite Swarm, *Journal of Guidance Control and Dynamics*, Vol. 30, No. 2, March-April 2007, pp. 449-459.

[11] P. Guan, X.J. Liu and J.Z. Liu, Flexible Attlitude Control Via Sliding Mode Technique, *Proceedings of the* 45^{th} *IEEE Conference on Decision and Control*, IEEE Publications, 2005, pp. 1258-1263.

[12] H. Wong, H. Pan, V. Kapila, Output Feedback Control For Spacecraft Formation Flying With Coupled Translation and Attitude Dynamics, *2005 American Control Conference*, June 8-10, 2005, portland, USA.

[13] H. Pan and V. Kapila, Adaptive Nonlinear Control For Spacecraft Formation Flying With Coupled Translational and Attitude Dynamics, *Proceedings of the* 40^{th} *IEEE Conference on Descision and Control*, IEEE Publications, December 2001, pp. 2057-2062.

[14] F. Terui, Position and Attitude Control of a Spacecraft by Sliding Mode Control, *Proceedings of the American Control Conference*, AACC Publications, June 1998, pp. 217-221.

[15] O. Fjellstad and T.I. Fossen, Quaternion Feedback Regulation of Underwater Vehicles, *Proceedings of the 3rd IEEE Conference on Control Application*, Glasgow, Scotland, U.K., Aug. 24-26, 1994, pp. 857-862.

[16] O. Khatib, Real-time Obstacle Avoidance for Manipulators and Mobile Robots, *Int Journal of Robotics Research*, Vol 5 No2, 1986, pp. 90-98

[17] C. McInnes, Autonomous rendezvous Using Artificial Potential Functions, *Journal of Guidance Control and Dynamics*, Vol. 18 No.2, 1995, pp. 237-241

[18] H. Chang, A New Technique to Handle Local Minimum for Imperfect Potential Field Based Path Planning, *Proceedings of the IEEE International Conference on Robotics and Automation*, Vol 1, IEEE, 1996 pp. 108-112.

[19] K. Sato, Dead-Lock Motion Path Planning Using The Laplace Potential Field, *Advanced Robotics*, Vol 17, No. 5, 1993, pp. 449-461.

[20] D. Keymeulen and J. Decuyper, The Fluid Dynamics Applied to Mobile Robot Motion: The Stream Field Method, *Proceedings of the IEEE International Conference on Robotics and Automation*, IEEE Publications, 1994, pp. 378-386.

[21] J.Y. Hung, W. Gao and J.C. Hung, Variable Structure Control: A Survey, *IEEE Transactions On Industrial Electronics*, Vol. 10, No. 1, February 1993, pp. 2-22.

[22] R.A. DeCarlo, S.H. Zak and G.P. Matthews, Variable Structure Control of Nonlinear Multivariable Systems: A Tutorial, *Invited Paper, Proceedings of the IEEE*, Vol. 76, No. 3, March 1988, pp.212-232.

[23] Bong Wie, Space Vehicle Dynamics And Control, *AIAA Education Series*, ISBN: 1-56347-261-9.

[24] J.E. Slotine and W. Li, Applied Nonlinear Control, *Prentice Hall Publications*, ISBN: 0-13-040890-5.

[25] M. Wooldridge, An Introduction to MultiAgent Systems, *John Wiley & Sons Ltd*, ISBN: 0-471-49691-X.

[26] M.J. Sidi, Spacecraft Dynamics and Control: A Practical Engineering Approach, *cambridge University Press*, ISBN: 0-521-78780-7

[27] The Herschel Science Mission [Online], Available at http://sci.esa.int/science-e/www/object/index.cfm?fobjectid=34682

[28] The Terrestrial Planet Finder Misssion [Online], Available at http://planetquest.jpl.nasa.gov/TPF

[29] The Micro Arc-Second X-Ray Imaging Mission (MAXIM) [Online], Avaiable at http://maxim.gsfc.nasa.gov

[30] The International Sun-Earth Explorer 3 (ISEE-3) [Online], Available at http://heasarc.nasa.gov/docs/heasarc/missions/isee3.html

[31] The Solar and Heliospheric Observatory (SOHO) [Online], Available at http://sohowww.nascom.nasa.gov/